IMMEDIATE COMMUNICATION OPEN

Check for updates

Effect of non-invasive spinal cord stimulation in unmedicated adults with major depressive disorder: a pilot randomized controlled trial and induced current flow pattern

Francisco Romo-Nava[1,2]✉, Oluwole O. Awosika[3], Ishita Basu[4], Thomas J. Blom[1,2], Jeffrey Welge[2,5], Abhishek Datta[6], Alexander Guillen[6], Anna I. Guerdjikova[1,2], David E. Fleck[2], Georgi Georgiev[1], Nicole Mori[1,2], Luis R. Patino[2], Melissa P. DelBello[2], Robert K. McNamara[2], Ruud M. Buijs[7], Mark A. Frye[8] and Susan L. McElroy[1,2]

Converging theoretical frameworks suggest a role and a therapeutic potential for spinal interoceptive pathways in major depressive disorder (MDD). Here, we aimed to evaluate the antidepressant effects and tolerability of transcutaneous spinal direct current stimulation (tsDCS) in MDD. This was a double-blind, randomized, sham-controlled, parallel group, pilot clinical trial in unmedicated adults with moderate MDD. Twenty participants were randomly allocated (1:1 ratio) to receive "active" 2.5 mA or "sham" anodal tsDCS sessions with a thoracic (anode; T10)/right shoulder (cathode) electrode montage 3 times/week for 8 weeks. Change in depression severity (MADRS) scores (prespecified primary outcome) and secondary clinical outcomes were analyzed with ANOVA models. An E-Field model was generated using the active tsDCS parameters. Compared to sham ($n = 9$), the active tsDCS group ($n = 10$) showed a greater baseline to endpoint decrease in MADRS score with a large effect size (-14.6 ± 2.5 vs. -21.7 ± 2.3, $p = 0.040$, $d = 0.86$). Additionally, compared to sham, active tsDCS induced a greater decrease in MADRS "reported sadness" item (-1.8 ± 0.4 vs. -3.2 ± 0.4, $p = 0.012$), and a greater cumulative decrease in pre/post tsDCS session diastolic blood pressure change from baseline to endpoint (group difference: 7.9 ± 3.7 mmHg, $p = 0.039$). Statistical trends in the same direction were observed for MADRS "pessimistic thoughts" item and week-8 CGI-I scores. No group differences were observed in adverse events (AEs) and no serious AEs occurred. The current flow simulation showed electric field at strength within the neuromodulation range (max. ~0.45 V/m) reaching the thoracic spinal gray matter. The results from this pilot study suggest that tsDCS is feasible, well-tolerated, and shows therapeutic potential in MDD. This work also provides the initial framework for the cautious exploration of non-invasive spinal cord neuromodulation in the context of mental health research and therapeutics. The underlying mechanisms warrant further investigation. Clinicaltrials.gov registration: NCT03433339 URL: https://clinicaltrials.gov/ct2/show/NCT03433339.

Molecular Psychiatry; https://doi.org/10.1038/s41380-023-02349-9

INTRODUCTION

Spinal interoceptive pathways (SIPs) convey a constant flux of information to the brain about bodily states [1]. Longstanding theoretical frameworks propose that SIPs, the corticocortical connections and the associated Bayesian active inference interoceptive processes in the brain regulate bodily states through descending projections [2–7]. These interoceptive processes and predictions play a critical role in emotional experience and are therefore key to the concept of mood and mood disorders like major depressive disorder (MDD) [1, 2, 4–6, 8–13]. Evidence from clinical [14] and imaging studies supports that regions within a distributed interoceptive system in the brain (e.g., insular cortex) integrate and process interoceptive signals [7] and are involved in the pathophysiology of MDD [4, 13–19]. However, the role of SIPs and their potential as therapeutic targets in MDD are unknown.

SIPs are a crucial afferent component of a brain-body interaction circuit [1]. SIPs include the unmyelinated C fibers and myelinated Aδ afferent fibers carrying somatic (e.g., pain, temperature, itch) and visceral sensory information that enters the spinal cord via the dorsal root ganglions and synapse to second-order neurons in the spinal dorsal horns (e.g., lamina I) [20, 21]. These fibers project to autonomic centers in the brainstem [2] and thalamus [10, 11]. Information is then relayed to a distributed interoceptive system in subcortical and cortical areas including the insular cortex [2, 7, 22]. In the insular cortex, interoceptive signals are organized somatotopically with a posterior-to-anterior gradient and entwined with motivational and cognitive processes interacting with other brain regions [4, 11]. The insula is recognized as a critical integrative hub for interoceptive signals involved in a myriad of functions including

[1]Lindner Center of HOPE, Mason, OH, USA. [2]Department of Psychiatry and Behavioral Neuroscience, University of Cincinnati College of Medicine, Cincinnati, OH, USA. [3]Department of Neurology and Rehabilitation Medicine, University of Cincinnati College of Medicine, Cincinnati, OH, USA. [4]Department of Neurosurgery, University of Cincinnati College of Medicine, Cincinnati, OH, USA. [5]Department of Environmental and Public Health Sciences, University of Cincinnati College of Medicine, Cincinnati, OH, USA. [6]Research and Development, Soterix Medical, Inc, New York, NY, USA. [7]Departamento de Fisiología Celular y Biología, Instituto de Investigaciones Biomédicas, Universidad Nacional Autónoma de México, México City, México. [8]Department of Psychiatry and Psychology, Mayo Clinic, Rochester, MN, USA. ✉email: romofo@ucmail.uc.edu

Received: 30 May 2023 Revised: 20 November 2023 Accepted: 27 November 2023
Published online: 20 December 2023

sensorimotor, reward, emotion, and pain processing [11, 23–25]. According to predictive processing and active inference interoceptive models, these signals act to generate, constrain, and update predictions about upcoming bodily states. These predictions reach efferent output regions such as the hypothalamus [4, 26–28], enabling the brain to interact with the body through hormonal (e.g., hypothalamic-pituitary-adrenal axis) and neural (e.g., autonomic efferents) mechanisms to control physiological processes including sleep/wake cycles and biological rhythms, reproductive behavior, eating behavior, and cardiovascular and metabolic regulation [29–32]. The hypothalamus coordinates preautonomic neuronal systems connected to sympathetic and parasympathetic motor nuclei in the brainstem and spinal cord that innervate target organs [3, 30]. Finally, information from the body is conveyed back to SIPs, closing a brain-body circuit that maintains a delicate balance while adapting to allostatic loads and homeostatic demands.

Per current diagnostic criteria (e.g., *DSM-5*), core MDD symptoms include sadness, low or irritable mood and anhedonia, disturbed appetite, sleep, libido, and concentration, as well as negative thoughts about one's self and suicidal thoughts [33]. The current concept of MDD is that of a heterogeneous syndrome with multiple possible neurobiological components (e.g., hyperactive HPA axis and increased sympathetic tone), as well as contributing external factors (e.g., exposure to chronic stress) [34]. Often ignored, MDD in most patients is accompanied by unspecific autonomic and somatic symptoms involving multiple sensory modalities including pain conditions and abnormal body phenomena that further suggest disturbed interoceptive signaling and processing [12, 35]. This notion is supported by recent fMRI studies that have consistently reported a hypo-activation of the insular cortex during interoceptive tasks [19, 36] or resting-state in patients with MDD compared to healthy controls, and this has been proposed to be a state marker present during depressive episodes and remission [18]. Collectively, these observations suggest that chronically hyperactive/dysregulated efferent pathways and SIPs signaling may lead to anomalous interoceptive processing [4, 7, 13]. Consequently, a dysregulated brain-body circuit may be accessible to neuromodulation-based interventions targeting SIPs at the spinal cord level to explore their role and therapeutic potential in MDD.

Transcutaneous spinal direct current stimulation (tsDCS) is a novel, low-cost, and non-invasive tool to modulate spinal cord function in humans with potential to modulate SIPs [37–39]. Electric field (E-field) simulations with electrode montages where the anode is located at the level of T10 or T11 spinous process and the cathode on the shoulder show that currents between 2.5 and 3.0 mA effectively reach the spinal cord with an E-Field maximum strength in the range of 0.47 to 0.82 V/m [40, 41]. This is above the commonly used 0.15 V/m threshold for neuromodulation in the cortex and in range to potentially induce synaptic plasticity (~0.75 V/m) [42–44]. In addition, a thoracic (T10)-shoulder electrode montage with anodal tsDCS is inhibitory to SIPs [37–39] and induces supraspinal brain function changes in MDD-relevant regions, including the thalamus and insular cortex [45–48]. Moreover, tsDCS is generally well-tolerated with some participants only reporting transient itch or burning sensation or erythema at electrode placement sites. To our knowledge, no published study on tsDCS has reported associated serious adverse events, and currents utilized are well below the known thresholds to induce tissue damage (~25 mA) [49].

Historically, the scarcity of tools to investigate or modulate spinal pathways in humans with MDD have limited our understanding of the contribution of SIPs to the depressive syndrome. Here, we hypothesized that an altered brain-body interaction contributes to the pathophysiology of MDD and that inhibition of spinal afferent (e.g., SIPs) signaling via repeated thoracic anodal tsDCS would decrease depressive symptom severity. As an initial test of our hypothesis, we evaluated the effects and tolerability of tsDCS in unmedicated adults with MDD in a pilot randomized sham-controlled clinical trial.

METHODS AND MATERIALS

This was an 8-week, double-blind, randomized, parallel group, sham-controlled pilot clinical trial. The protocol was approved by the University of Cincinnati Institutional Review Board and was conducted in accordance with the Declaration of Helsinki and following EQUATOR (CONSORT) reporting guidelines [50]. All study procedures involving participants were conducted at the Lindner Center of HOPE (affiliated with the University of Cincinnati) in Mason, Ohio, with a recruitment period from August 29, 2018, to September 13, 2022. The clinical trial was registered at clinicaltrials.gov registration number NCT03433339.

Participants

Eligible individuals were recruited from the community and from the Lindner Center of HOPE through advertising and word of mouth. All participants signed an informed consent form prior to initiate study procedures.

Inclusion criteria included. (1) age 18–55 years, inclusive; (2) female or male sex; (3) BMI 18.5 to 35 kg/mts^2; (4) current MDD episode diagnosis confirmed by Mini International Neuropsychiatric Interview (MINI) 5.0 with a duration of ≥1 month and ≤24 months; (5) moderate MDD symptom severity defined by a Montgomery-Asberg Depression Rating Scale (MADRS) score ≥20 to ≤35; (6) no current or recent (past month) antidepressant pharmacological treatment; and (7) in all participants of childbearing potential, use of an effective contraceptive method. Exclusion criteria included: (1) current or lifetime MDD episode non-responsive to two or more antidepressant treatments at adequate doses and time (including electroconvulsive therapy or other neuromodulation-based treatment); (2) lifetime bipolar or psychotic disorder diagnosis; (3) current (past month) post-traumatic stress disorder or substance use disorder (nicotine use, generalized anxiety and other anxiety symptoms were allowed); (4) significant risk of suicide according to the Columbia Suicide Severity Rating Scale (CSSRS) or clinical judgment, or suicidal behavior in the past year; (5) current chronic severe pain conditions; (6) current chronic use of: opioid analgesics, medications that affect blood pressure or drugs with significant autonomic effects (stimulants and antipsychotics were allowed if dose stable for >1 month); (7) neurological, endocrinological, cardiovascular (including diagnosed hypertension) or other clinically significant medical conditions; (8) skin lesions on electrode placement region; (9) implanted electrical medical devices; (10) pregnancy or breastfeeding; and (11) suspected IQ < 80.

Clinical assessments

The MINI 5.0 [51] was used to confirm the diagnosis of a current MDD episode and evaluate the presence of comorbid psychiatric disorders. The structured interview guide for the MADRS (primary outcome measure) was used to evaluate depressive symptom severity (at screening, baseline, weeks 1, 2, 4, 6, and 8) with total scores ranging from 0 to 60 [52, 53]. Baseline to last available observation change in MADRS total score was used to establish partial response (≥25% decrease from baseline), response (≥50% decrease from baseline), and remission (final MADRS score ≤9) rates [54]. The CSSRS [55] was used to evaluate suicidality. The clinical global impression-severity (CGI-S) and the clinical global impression-improvement (CGI-I) scales were used to evaluate the overall clinical severity and improvement of illness [56]. All clinical assessments, ratings, and interviews were conducted by trained clinicians from the team (F.R.N. or N.M.), with a MADRS Cronbach's alpha = 0.86.

Participants also completed self-report instruments as secondary outcomes. The Patient Health Questionare-9 (PHQ-9) was used as a secondary measure of depressive symptom severity [57]. Additionally, the Four-Dimensional Symptom Questionnaire (4DSQ) [58] was used to measure distress, somatization and anxiety symptoms; the Binge Eating Scale (BES) was used to measure eating behaviors and aspects of body perception [59]; and the multidimensional assessment of interoceptive awareness (MAIA) was utilized to measure interoceptive awareness [60]. Paper and/or electronic versions of the instruments were used. Data entry was conducted using Research Electronic Data Capture (REDCap, Vanderbilt University).

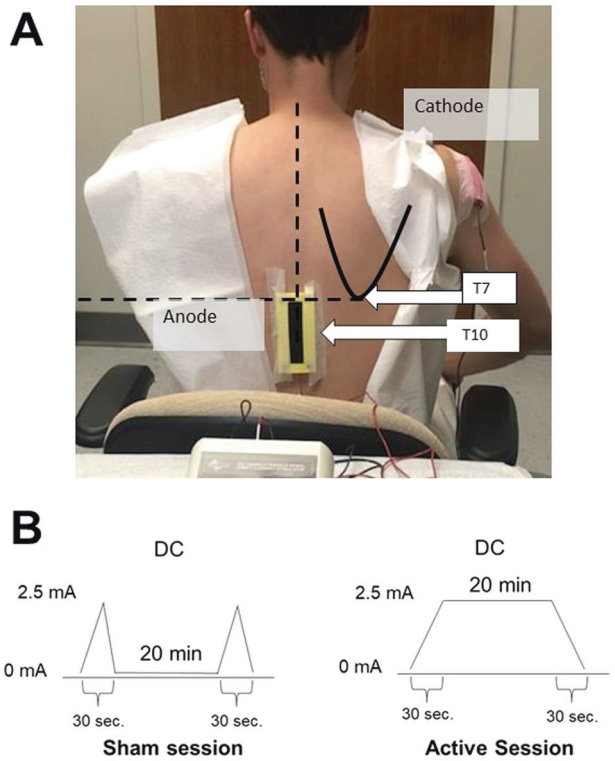

Fig. 1 Electrode montage and tsDCS temporal characteristics. For each participant, standard anatomical landmarks were identified for consistent electrode placement. With the participant sitting on a chair, a horizontal line traced medially from the inferior scapular angle identified the T7 spinous process level and then the T10 spinous process was identified through palpation of the spinous processes below. The center of the anode electrode sponge (vertical length) was placed at the level of the 10th vertebrae spinous process. The anode electrode was kept in place using adhesive surgical tape and contact with skin was enhanced by a lumbar BODYstrap (Soterix Medical®, New York, NY). The cathode (5 × 7 cm) electrode was placed on the right shoulder over the posterior deltoid area and was kept in place with adhesive surgical tape and an elastic arm band (**A**). The active stimulation induced a continuous anodal direct current (DC) gradually increased (within 30 s) to 2.5 mA during 20 min and then ramped down to 0 mA (within 30 s). The sham version induced a gradual current ramp up to 2.5 mA followed by a ramp down to 0 mA (within 30 s), kept at 0 mA for 20 min, and was followed by a final ramp up to 2.5 mA followed by a ramp down to 0 mA (within 30 s) (**B**). Photo published with consent.

Intervention

At baseline, participants were randomized to receive either "sham" or "active" tsDCS sessions 20 min each, three times/week, during weekday office hours for 8 weeks. Participants could receive sessions on no more than two consecutive days per week. The tsDCS device 2 × 2 transcutaneous spinal direct current stimulator model 0707-A (Soterix Medical®, New York, NY) was utilized. This device is available in the US only for investigational use and was labeled accordingly.

In preparation for each tsDCS session, participants were asked to change into a gown and remain seated. Carbon rubber electrodes (4.5 × 4.5 cm) were placed inside EASYpad sponges (Soterix Medical ®) moist in saline solution (0.9% NaCl) to decrease impedance. The sponge size for the anode electrode was 5 × 10 cm and the cathode was 5 × 7 cm. The electrodes were connected to the tsDCS device through cables 188 cm in length. A detailed description of the electrode montage and tsDCS temporal characteristics are presented in Fig. 1.

The protocol allowed for a current dose decrease to 2.0 or 1.5 mA if stimulation intensity was not tolerated at 2.5 mA. If a 1.5 mA current was not tolerated, the participant could be withdrawn from the study. If a participant tolerated a stimulation intensity of less than 2.5 mA, the study clinician could attempt to increase the dose to 2.0 mA or 2.5 mA when considered clinically appropriate. During the tsDCS sessions, subjects remained in a calm and relaxing environment. All participants were asked to conduct the same procedures and number of scheduled visits during the 8-week follow-up period.

Randomization and blinding

Participants were randomized in a 1:1 ratio (in blocks of four) using a simple allocation method to one of two experimental groups: (1) sham or (2) active anodal stimulation protocols. Randomization was double-blinded to participants and clinicians/raters. The allocation sequence was generated by a statistician not involved in other study procedures, handled by the device operator, and concealed from other members of the study team and participants until completion of statistical analysis of main outcomes.

An independent operator (trained personnel from the research team) prepared the tsDCS device active or sham setting for each session and did not participate in other assessments. After each session, the blinded clinician assessing AEs requested participants conceal temporal characteristics of expected sensations like itch or burning sensations to preserve blinding. Participants and raters remained blinded to the tsDCS protocol assigned to each participant throughout the study.

Autonomic parameters. Heart rate and blood pressure were obtained before and after 5 min of tsDCS sessions through the auscultatory technique on the left arm using a standard mercury sphygmomanometer in a sitting position and after 5 min of rest. An ECG tracing was obtained through standard 12-lead electrocardiography at screening, baseline, and weeks 4 and 8. Blood pressure and heart rate were considered as variables to assess autonomic function.

Anthropometric measures. Body mass index (BMI) was assessed on baseline, week 2, 4, 6 and 8.

Exploratory metabolic parameters. The effect of tsDCS on metabolic parameters regulated by brain-body interaction pathways including the autonomic nervous system and the gut-brain-axis were explored [32, 61–63]. Blood samples were obtained at baseline, and weeks 4 and 8 for serum adiponectin, leptin, cortisol, insulin and fibroblast growth factor-21 (FGF-21), and red blood cell long-chain omega-3 (LcN-3) fatty acids erythrocyte eicosapentaenoic acid (EPA) and docosahexaenoic acid (DHA) fatty acids levels. Samples were processed using ELISA assays at the Biochemistry Core Laboratory from the Schubert Research Clinic at Cincinnati Children's Hospital. Whole blood fatty acids were processed via gas chromatography at UC's Lipidomics Research Program as previously described [64]. Participants were asked to fast and blood draws were typically conducted at the time of the scheduled tsDCS session.

E-field simulation

Simulation of the induced electric field (E-field) due to the employed tsDCS montage was performed using a multi-step process that included (1) anatomical dataset and pre-processing, (2) electrode placement and meshing, and (3) finite element method (FEM) model generation and data analysis [65–67]. These steps ensure preservation of resolution of input anatomical data, were based on prior work, and are described in detail below [65, 66]. Consistent with prior tsDCS E-field simulation models, an E-field strength >0.15 V/m was considered as the threshold for neuromodulation [41, 68].

(1) Anatomical dataset and pre-processing
The 3D-anatomical dataset corresponded to the Duke human model from the Virtual Population (ViP) 2.0 model database, a set of detailed high-resolution anatomical models created from magnetic resonance image data of volunteers [69]. Description of the dataset is summarized in Supplementary Table 1. This model version includes a total of 22 tissues/tissue groups and include the following: skull, tongue, cerebrospinal fluid, cerebrum (gray matter), cerebrum (white matter), cerebellum, thalamus, brain stem, spinal cord, spinal nerves, spinal gray matter, bone, muscle, cartilage, respiratory system, heart, gastrointestinal system, liver, kidney, bladder, reproductive system, and other tissues. The Duke dataset was imported into Simpleware (Synopsys Ltd, CA, USA) to correct for anatomical and continuity errors as well as for additional processing (step 2 and 3).

(2) Electrode placement and meshing
Anode and cathode electrodes were modeled in Simpleware, mimicking the $7 \times 10\ cm^2$ and $5 \times 7\ cm^2$ rectangular pads used in our clinical trial. Each electrode was simulated as a conductor interfaced with the anatomical geometry with a similar sized geometry mimicking the saline compartment. One conductor-saline combination was placed at the level of the T10 process, with the second conductor-saline combination on the right shoulder. The entire model (anatomical masks and electrodes) was adaptively meshed using Simpleware.

(3) Finite element method (FEM) model generation and data analysis
The mesh was then imported into COMSOL Multiphysics 5.6 (COMSOL Inc., MA, USA) to develop a FEM model for computing induced current flow. The isotropic and homogeneous electrical conductivity value in S/m assigned to each mask were: skull (0.01), tongue (0.35), cerebrospinal fluid (1.65), cerebrum (gray matter) (0.276), cerebrum (white matter) (0.126), cerebellum (0.276), thalamus (0.276), brain stem (0.276), spinal cord (0.2), spinal nerves (0.276), spinal gray matter (0.276), bone (0.01), muscle (0.35), cartilage (1.01), respiratory system (0.05), heart (0.381), gastrointestinal system (0.164), liver (0.221), kidney (0.403), bladder (0.408), reproductive system (0.232), other tissues (0.465), sponge: 1.4; and electrode: 5.9 e7 [69]. The model was solved under quasi-static assumption, and thus a value of 1 was assigned for the relative permittivity for all tissue domains. The model physics was formulated with the standard Laplace equation with the following boundary conditions: (1) normal current density condition for the electrode at T10 corresponding to 2.5 mA (anode), (2) ground for shoulder electrode (cathode), and (3) all external surfaces treated as insulated. The conjugate gradient solver is used for computation with the tolerance for convergence set at: 1e−6. The final model consisted of 16,231,185 tetrahedron elements with 22,333,066 degrees of freedom. Post computation, we analyzed 3D surface and 2D cross-sectional (axial) induced E-field plots on the spinal cord.

Outcomes

The prespecified primary outcome was the difference in change from baseline to week 8 (or last available observation) in MADRS total score between active and sham tsDCS groups. The prespecified secondary outcomes were difference in baseline to endpoint change in MADRS subcomponent scores, clinical measures (CGI-I, CGI-S, PHQ-9, MAIA, BES and 4DSQ), autonomic measures (BP, HR), and metabolic parameters. Secondary outcomes also included the correlation between change from baseline to last available observation in MADRS scores, and BMI and autonomic (BP, HR) change from baseline to last available observation, as well as the differences in adverse event frequency occurring from baseline to endpoint between active and sham tsDCS groups.

Adverse events

Adverse events were evaluated before and after each tsDCS session and during the completion of baseline, week 1, 2, 4, 6 and 8 visits through open-ended questions. Physical and neurological examinations were conducted at baseline, week 1, 2, 4, and 8 to assess for AEs. Participants were also instructed to report any potential adverse events that occurred in-between visits or after study completion.

Statistical analysis

The prespecified recruitment goal for this proof-of-concept study was set to 20 participants (10 per group). This sample size selection was considering that estimates of effect sizes would be useful as inputs to larger confirmatory studies if the effects fell in an appropriate range (i.e., at least moderate sample effect sizes of ~0.5 standard deviations). Participants with at least one post-baseline assessment were included in the analysis according to treatment allocation groups [70]. Baseline comparisons on clinical variables were conducted using two-sample *t*-tests, allowing for heterogenous group variance. Longitudinal analyses were performed using repeated measures ANOVA models using all available data. The models used an autoregressive covariance structure to account for within-participant correlation in the data. All missing data were considered to be missing at random and there was no evidence in the data that would contradict this assumption. For example, for the primary outcome measure, the mixed ANOVA models used all visits in the model estimates with the a priori primary analysis examining change in MADRS from baseline to week 8. Pearson correlations were used to assess the relationships between change in MADRS, from baseline to endpoint, and baseline BMI and change from baseline to endpoint in pre/post tsDCS session blood pressure. Throughout, tests and confidence intervals for effect sizes were two-sided, $\alpha = 0.05$. The effect size for the primary outcome was estimated using Cohen's *d* traditional cutoffs for small, medium, or large effects sizes (0.2, 0.4, and 0.8, respectively).

RESULTS

We pre-screened 671 potential candidates by phone through an IRB-approved questionnaire. Forty-two participants were screened on site, and 20 individuals with MDD were randomized to receive sham ($n = 10$) or active ($n = 10$) anodal tsDCS sessions at a 2.5 mA current at a frequency of three per week for 8 weeks. Nineteen participants had at least one MADRS assessment after baseline (active, $n = 10$, and sham, $n = 9$) and were included in the analysis (see CONSORT diagram in Supplementary Fig. 1).

Six participants discontinued treatment before week 8 for an attrition rate of 30% (sham = 4, active = 2). In the sham group, 1 withdrew after the first session to seek other treatment options, 2 at week 4 due to COVID-19 pandemic related restrictions, and 1 at week 5 due to "personal reasons". In the active group, 1 withdrew at week 2 and 1 at week 4 (both were lost to follow up). The latter was a young athletic female with a baseline sinus bradycardia that was referred for evaluation about her continuation on the study due to a further asymptomatic decrease in heart rate and was lost to follow up (Supplementary Case Detail 1). Six (60%) sham-receiving participants and 8 (80%) active tsDCS-receiving participants completed the 8-week trial. In addition, out of 24 scheduled tsDCS sessions, participants in the active group received a mean (SD) of 19.3 (5.9) tsDCS sessions, similar to the 18.7 (4.7) sessions received by the sham group ($p = 0.80$). There were no differences in baseline demographics or clinical characteristics between the active and sham groups, including MADRS scores, MDD episode duration, and time since last treatment (Table 1). No participant was on a stimulant, antipsychotic or other psychotropic medication during the study.

Primary outcome

Compared to sham, the least squares (LS) mean (±SE) in MADRS total score decrease from baseline to week 8 was greater in the active group with a large effect size (-14.6 ± 2.5 vs. -21.7 ± 2.3, $p = 0.040$, Cohen's $d = 0.86$). Grouped and individual raw MADRS total scores are shown in Fig. 2A, B.

Secondary and exploratory outcome

Clinical measures. Categorical response rate differences between the intervention groups according to MADRS score did not reach statistical significance for partial response ($p = 0.08$), response ($p = 0.36$), or remission ($p = 0.34$) criteria (Supplementary Table 2). A MADRS item-level analysis showed that compared to sham, active tsDCS induced a greater decrease in LS mean (±SE) MADRS "reported sadness" item (-1.8 ± 0.4 vs. -3.2 ± 0.4, $p = 0.012$). A statistical trend in the same direction was observed for "pessimistic thoughts" item (-0.8 ± 0.5 vs. -1.9 ± 0.4, 0.094), as well as week-8 clinical global impression-improvement (CGI-I) scale scores (2.0 ± 0.3 vs. 1.3 ± 0.3, $p = 0.091$). Although greater numerical decreases in the active group were observed on all MADRS items (except "reduced sleep"), no other statistically significant difference was observed between groups. There were no significant differences in change from baseline to week 8 between intervention groups on self-reported PHQ-9, MAIA, 4-DSQ, and BES scales (Table 2).

Table 1. Baseline demographics and clinical characteristics.

	Sham ($n = 9$)	Active ($n = 10$)	p value
Age, years	36.8 (13.1)	31.6 (9.8)	0.339
Sex, female	4 (44%)	8 (80%)	0.170
Race, white	8 (89%)	8 (80%)	1.000
MADRS	29.4 (3.8)	29.0 (2.3)	0.759
Time since last treatment, months	38.0 (26.1)	57.2 (78.)	0.503
Current MDD duration, months	10.2 (7.5)	6.0 (6.4)	0.209
CGI-S	4.1 (0.3)	4.2 (0.4)	0.620
PHQ-9	16.2 (4.7)	16.3 (4.1)	0.970
BES	8.4 (7.2)	13.8 (11.7)	0.254
MAIA—Noticing	3.2 (0.7)	3.1 (0.9)	0.753
MAIA—Not-distracting	2.3 (0.8)	2.2 (1.4)	0.808
MAIA—Not-worrying	3.1 (1.0)	3.1 (1.1)	0.905
MAIA—Attention regulation	2.7 (0.8)	2.5 (1.0)	0.695
MAIA—Emotional awareness	3.1 (1.0)	3.4 (1.1)	0.639
MAIA—Self-regulation	2.6 (1.0)	2.2 (0.8)	0.309
MAIA—Body listening	2.0 (1.1)	1.5 (1.0)	0.325
MAIA—Trusting	3.1 (1.2)	2.6 (1.4)	0.378
4DSQ—Somatization	8.1 (8.4)	7.0 (4.5)	0.710
4DSQ—Distress	21.1 (4.1)	20.7 (5.2)	0.856
4DSQ—Anxiety	7.2 (4.9)	4.9 (2.8)	0.214
4DSQ—Depression	4.3 (2.8)	5.7 (4.2)	0.424
Systolic. BP, pre-session	116.4 (12.7)	114.2 (5.3)	0.632
Diastolic. BP, pre-session	80.1 (6.7)	77.8 (5.5)	0.423
Pulse (pre-session)	67.9 (5.4)	70.6 (7.9)	0.400
ECG—QTcB	406.3 (19.2)	414.8 (17.6)	0.330
BMI	25.6 (4.3)	25.2 (4.8)	0.847
Adiponectin	14,433 (6465)	15,246 (13,232)	0.870
FGF-21	142.2 (217.5)	200.0 (308.3)	0.647
Leptin	16.8 (13.3)	23.3 (18.3)	0.389
LCn-3	4.8 (1.2)	5.3 (1.5)	0.454
Insulin	13.4 (10.8)	12.4 (14.8)	0.874
Cortisol	10.8 (5.1)	12.2 (4.8)	0.531

Mean (SD) or *n* (%) shown.
tsDCS transcutaneous spinal direct current stimulation, *MADRS* Montgomery Asberg Depression Rating Scale, *CGI-I* Clinical Global Impression-Improvement, *PHQ-9* Patient Health Questionnaire-9, *BES* Binge Eating Scale, *MAIA* Multidimensional Assessment of Interoceptive Awareness, *4-DSQ* Four-Dimensional Symptom Questionnaire, *BP* blood pressure, *ECG* electrocardiogram, *QTcB* QT correction with Bazzett formula, *BMI* body mass index, *FGF-21* fibroblast growth factor-21.

Autonomic and metabolic outcomes. No group differences were observed for baseline to week 8 change in pre-tsDCS session BP, HR, or QtcB. Autonomic outcomes were also analyzed for differences in pre/post session changes from baseline to endpoint between groups (Table 2). Compared to sham, active tsDCS induced a greater decrease in diastolic BP pre/post session change from baseline to endpoint with a LS mean (±SE) group difference (7.9 ± 3.7 mmHg, DF = 70, *t*-value = 2.1, $p = 0.039$). No difference was observed in pre/post tsDCS session change from baseline to endpoint in systolic BP (6.2 ± 3.9, DF = 70, *t*-value = 1.57, $p = 0.12$) or heart rate (4.8 ± 3.1, DF = 70, *t*-value = 1.53, $p = 0.13$). Longitudinal pre/post tsDCS session BP and HR values are presented in Fig. 2C–E.

When all participants were analyzed in a single group, a statistically significant positive correlation between MADRS score baseline to endpoint change was observed with baseline to week 8 pre/post tsDCS session change in systolic BP ($r = 0.54$, $p = 0.016$) (Supplementary Fig. 2 and Supplementary Table 3), with a statistical trend in the same direction for diastolic BP ($r = 0.45$, $p = 0.056$) (Supplementary Table 3). However, no statistically significant correlation was observed between these parameters when analyzing the active and sham groups individually (Supplementary Table 3).

No group differences were observed in baseline to week 8 changes on BMI or exploratory metabolic parameters adiponectin, FGF-21, leptin, RBC (EPA + DHA), insulin or cortisol (Supplementary Table 4). No correlation was observed between baseline BMI and change in MADRS scores.

Adverse events

No group differences were observed in baseline to endpoint AEs frequency. All participants receiving tsDCS at 2.5 mA reported that it was well-tolerated, and no lowering of electrical current dose protocols were required. In both sham and active groups, the most common AEs were occasional mild transient erythema (redness) after tsDCS sessions (typical duration <30 min) or mild, transient, non-painful itch or burning sensation on either the thoracic and/or shoulder electrode sites during the sessions (Table 3). There were no serious adverse events.

E-Field modeling

The E-field model generated with the active tsDCS parameters and electrode montage of this study shows that the current effectively reaches the thoracic spinal cord gray matter with an E-field strength up to 0.45 V/m, which is above the reported threshold for neuromodulation in the cortex (>0.15 V/m). The E-field strength above the thoracic spinal cord gray matter does not reach the neuromodulation threshold (Fig. 3).

DISCUSSION

In this proof-of-concept randomized double-blinded clinical trial, we observed that compared to sham, active thoracic anodal tsDCS induced a statistically significant greater decrease in depressive symptom severity among moderately ill individuals with MDD with a large effect size. Compared to sham, tsDCS also induced a greater decrease in MADRS Item 2 (reported sadness) and a statistical trend in the same direction was observed for Item 9 (pessimistic thoughts), as well as week-8 CGI-I scale scores. Active tsDCS also induced a cumulative decrease in pre/post tsDCS session diastolic blood pressure. The intervention was well-tolerated and no serious AEs were observed. The E-field simulation generated with the active tsDCS parameters indicate that the applied current was sufficient to reach the SIPs as putative anatomical targets in the thoracic spinal gray matter at E-field strengths within neuromodulation range. Hence, these results are consistent with our hypothesis that spinal brain-body interaction pathways that include SIPs may play a relevant role in MDD pathophysiology and warrant further study as potential novel therapeutic targets for neuromodulation with tsDCS. Albeit encouraging, results from this pilot feasibility study should be considered preliminary and interpreted with caution considering all limitations and pending corroboration from larger definitive studies.

The mechanisms of action for the observed effects of tsDCS in MDD are yet to be determined. Preliminary evidence suggests

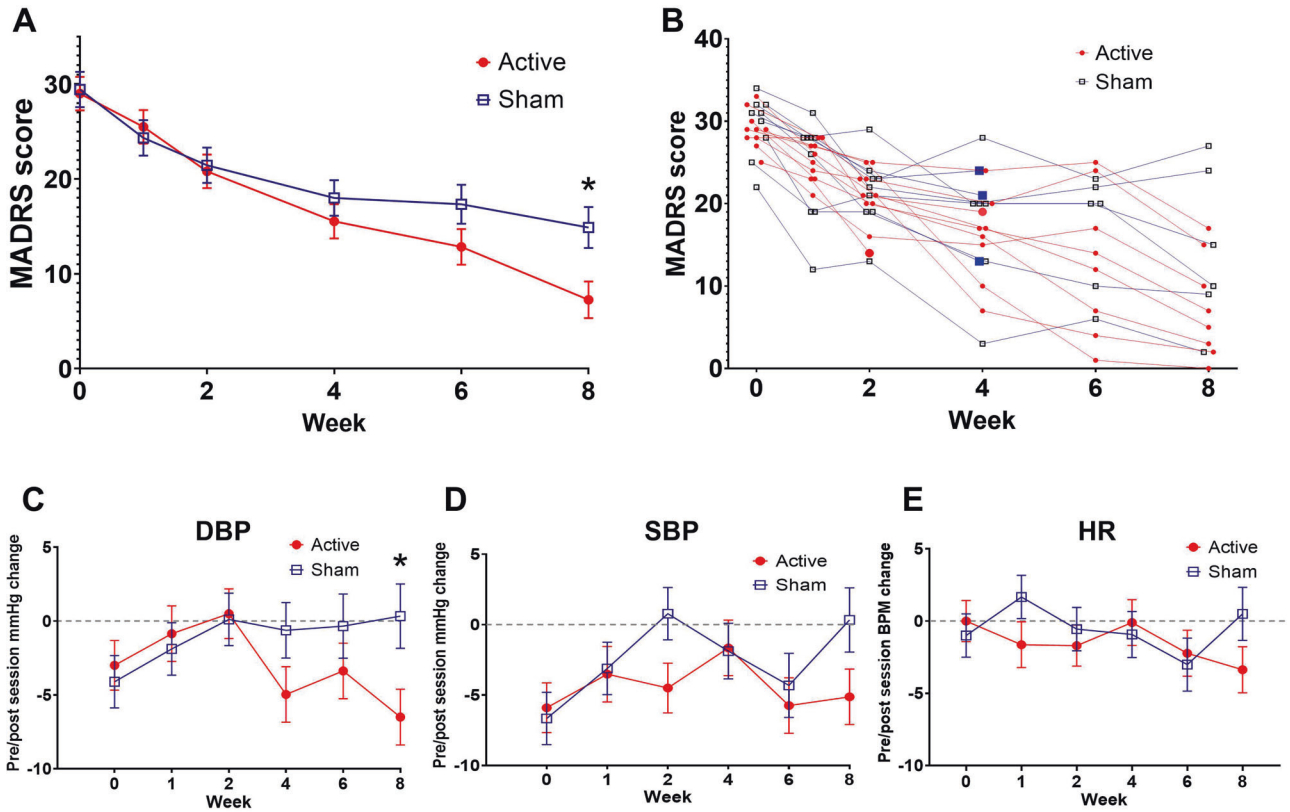

Fig. 2 Longitudinal MADRS scores and pre/post session changes in blood pressure (BP) and heart rate. Grouped mean with standard error bars are presented for baseline to last available observation MADRS scores (**A**). Individual raw MADRS scores from baseline to last available observation for all participants included in the analysis on both intervention groups with an enlarged marker (red circles for active, blue squares for sham) identifying the last available assessment for individuals that discontinued participation early (**B**). Grouped mean with standard error bars are presented for baseline to last available observation change in pre/post tsDCS session values for diastolic (**C**) and systolic (**D**) BP, and heart rate (**E**) for each intervention group. * Mixed ANOVA model between group difference $p < 0.05$.

that these may involve local inhibition of SIPs at the level of the spinal dorsal horns (and other spinal afferents) [37, 71] through low-magnitude electric fields [72, 73] resulting in supraspinal effects on integrative brain regions [45–48]. The cumulative tsDCS session after-effects on diastolic BP may also signal an effect on efferent pathways through local or supraspinal loops [73]. However, our study design and results are insufficient to clarify such complex mechanisms. Future in-depth assessment of the effects of tsDCS on spinal afferent and efferent pathways, as well as on MDD-relevant brain regions are warranted to determine the role of the distributed interoceptive system in MDD [4, 13–19] and the therapeutic potential of non-invasive spinal cord stimulation.

As noted above, the observed longitudinal decrease in pre/post session changes from baseline to endpoint suggests a cumulative tsDCS time-dependent after-effect on autonomic function that may involve neuroplastic processes on afferent, and possibly efferent pathways [72]. The lack of a discernible longitudinal effect of active tsDCS on resting BP, HR or QtcB measurements compared to sham provides preliminary evidence for cardiovascular safety. The on-line and after-effects of tsDCS on autonomic parameters, their duration, and their value as potential target engagement markers warrants further investigation.

It is important to highlight the limitations of this study. The sample size was small and may play a role in the observed effect size. It is currently unknown if the T10/shoulder electrode montage is optimal and whether other montages (e.g., other thoracic or cervical levels) may show a different efficacy or safety profile. Optimal electrode montage, session frequency, and dose-finding studies are needed to confirm the potential of tsDCS as monotherapy and/or as an adjuvant intervention in MDD. In addition, the study design is not sufficient to evaluate the exact mechanisms of action of tsDCS and these should be evaluated in future studies. For example, objective assessments that evaluate target engagement of SIPs [37–39] in combination with the evaluation of direct or indirect effects on interoceptive processes [12], as well as measures of efferent autonomic function could contribute to untangle brain-body interaction mechanisms involved in acute and long-term tsDCS effects in MDD. Moreover, the sizeable "sham" response could suggest a physiological effect and supports the exploration of alternative "sham" versions (e.g., lower peak current ramp up) in future studies to minimize this while ensuring blinding.

In addition to the procedures that we implemented to protect blinding, additional strategies could be considered to maintain successful masking in future studies. For example, AE profile and physiological effects may represent a risk to masking in larger clinical trials and warrant attention. In this study, AEs were similar between the intervention groups, but the presence of skin redness showed a statistical trend towards being more frequent on the active compared to the sham group. In this case, the risk to blinding is mitigated by the presence of skin redness in 4 out of 9 of participants in the sham group, and the observation that not all participants (9 out of 10) on the "active" group developed skin redness. Nonetheless, skin redness may require evaluation as a potential risk to intervention blinding in future studies [74]. Specifically, this should be considered when exploring a lower sham current ramp up (compared to the active version), as it may

Table 2. Analysis of clinical and autonomic outcomes.

	Sham	Active	*p* value
Study tsDCS visits completed	18.7 (4.7)	19.3 (5.9)	0.800
MADRS, LS mean change (SE) Week 8-BL	−14.6 (2.5)	−21.7 (2.3)	**0.040**
Item 1. Apparent sadness	−2.1 (0.5)	−2.8 (0.5)	0.271
Item 2. Reported sadness	−1.8 (0.4)	−3.2 (0.4)	**0.012**
Item 3. Inner tension	−1.4 (0.5)	−1.9 (0.4)	0.419
Item 4. Reduced sleep	−1.3 (0.7)	−0.9 (0.6)	0.687
Item 5. Reduced appetite	−0.5 (0.6)	−0.9 (0.5)	0.565
Item 6. Concentration difficulties	−1.8 (0.6)	−2.6 (0.5)	0.308
Item 7. Lassitude	−1.7 (0.5)	−2.6 (0.5)	0.213
Item 8. Inability to feel	−2.0 (0.5)	−2.8 (0.4)	0.188
Item 9. Pessimistic thoughts	−0.8 (0.5)	−1.9 (0.4)	0.094
Item 10. Suicidal thoughts	−1.4 (0.3)	−1.9 (0.3)	0.271
CGI-I, LS mean (SE) at Week 8	2.0 (0.3)	1.3 (0.3)	0.091
PHQ-9, LS mean change (SE) Week 8-BL	−10.3 (2.4)	−12.6 (2.2)	0.472
BES, LS mean change (SE) Week 8-BL	−3.0 (3.0)	−7.3 (2.7)	0.300
MAIA—Noticing	−0.2 (0.5)	−0.0 (0.5)	0.789
MAIA—Not-distracting	−0.2 (0.7)	0.2 (0.6)	0.694
MAIA—Not-worrying	−0.3 (0.5)	−0.1 (0.4)	0.799
MAIA—Attention regulation	−0.0 (0.5)	0.0 (0.4)	0.963
MAIA—Emotional awareness	−0.1 (0.6)	−0.1 (0.5)	0.981
MAIA—Self-regulation	0.3 (0.5)	0.6 (0.5)	0.692
MAIA—Body listening	0.5 (0.6)	1.0 (0.5)	0.514
MAIA—Trusting	0.4 (0.5)	0.7 (0.5)	0.745
4DSQ—Somatization	−6.9 (2.3)	−3.3 (2.1)	0.268
4DSQ—Distress	−13.4 (2.8)	−14.1 (2.5)	0.859
4DSQ—Anxiety	−5.1 (1.4)	−3.8 (1.2)	0.474
4DSQ—Depression	−3.6 (1.4)	−5.4 (1.2)	0.344
Systolic BP, LS mean change (SE) Week 8-BL	−2.9 (4.2)	−5.0 (3.9)	0.721
Diastolic. BP, LS mean change (SE) Week 8-BL	−0.6 (3.4)	2.1 (3.2)	0.553
Pulse, LS mean change (SE) Week 8-BL	5.3 (4.2)	4.7 (3.9)	0.921
ECG—QTcB	9.5 (7.0)	6.9 (6.2)	0.786
BMI	1.5 (2.2)	−0.3 (2.0)	0.540

Repeated measures ANOVA considering all available data. In bold *p* values <0.05.

tsDCS transcutaneous spinal direct current stimulation, *MADRS* Montgomery Asberg Depression Rating Scale, *LS* least squares, *SE* standard error, *BL* baseline, *CGI-I* Clinical Global Impression-Improvement, *PHQ-9* Patient Health Questionnaire-9, *BES* Binge Eating Scale, *MAIA* Multidimensional Assessment of Interoceptive Awareness, *4-DSQ* Four-Dimensional Symptom Questionnaire, *BP* blood pressure, *ECG* electrocardiogram, *QTcB* QT correction with Bazzett formula, *BMI* body mass index.

Table 3. Adverse events during study participation.

	Sham	Active	Fisher's exact *p* value
Anxiety/panic symptoms	1	1	1.00
Asymptomatic decrease in heart rate	0	1	1.00
Itching/Burning sensation	4	6	0.66
Cold-like symptoms	0	2	0.47
Cosmetic removal of Nevi and Acrochordon	1	0	1.00
COVID-19	0	1	1.00
Dermatitis	0	2	0.47
External ear infection	0	1	1.00
Friction blister in feet	1	0	1.00
Gastroenteritis	1	0	1.00
Headache	3	1	0.58
Pharyngitis	1	0	1.00
Prickling sensation	1	1	1.00
Rash	1	1	1.00
Skin abrasion	1	0	1.00
Skin redness (electrode sites)	4	9	0.06
Vaginitis	0	1	1.00

Table entries are number of patients with at least one occurrence.

result in less frequent skin redness or other AEs. These considerations apply to the observed post-tsDCS effects on autonomic parameters, or if autonomic effects during the tsDCS (online) are identified in future studies. To mitigate these risks, continuous and automated monitoring of autonomic/physiologic parameters may be implemented. Moreover, depending on the experimental design, future studies may consider using instruments to conduct a systematic evaluation of blinding of the intervention (e.g., adaptation of the credibility/expectancy questionnaire) [75]. Finally, as tsDCS devices continue to be developed, new versions could be equipped with automated and blinded sham/active allocation to eliminate the need for an unblinded operator.

Additional study limitations should be considered. For example, results showed no observable tsDCS effect on exploratory metabolic parameters, which should be interpreted with caution due to the small sample size, lack of control of time-of-day for blood extraction, as well as large within and interindividual variability. Likewise, eligibility criteria did not specify symptomatic domains (e.g., somatic symptoms, binge eating) which could contribute to the lack of group differences on self-reported instruments like the 4-DSQ, BES, and MAIA. In addition, this pilot study did not perform a follow-up visit after study procedures to evaluate duration of symptom relief and potential emergent AEs. When the efficacy, tolerability, and safety of tsDCS are thoroughly studied and confirmed, the development of "in-hospital (e.g., severe MDD)" or "at-home" tsDCS-based interventions could be explored to facilitate use, adherence, increase treatment duration, and mitigate attrition in clinical trials. In addition to tsDCS, cautious exploration of other invasive or non-invasive spinal cord modulation tools could provide mechanistic insight into complex constructs such as interoception, the neurobiological self, consciousness, MDD and other psychiatric disorders.

Collectively, this proof-of-concept study provides preliminary evidence that anodal thoracic tsDCS is feasible, well-tolerated, and has therapeutic potential in adults with MDD. Our findings also suggest that spinal pathways in MDD may represent a plausible new therapeutic target. Continued development of methods to modulate spinal pathways could further advance our understanding of brain-body interaction and interoceptive processes in psychiatric disorders.

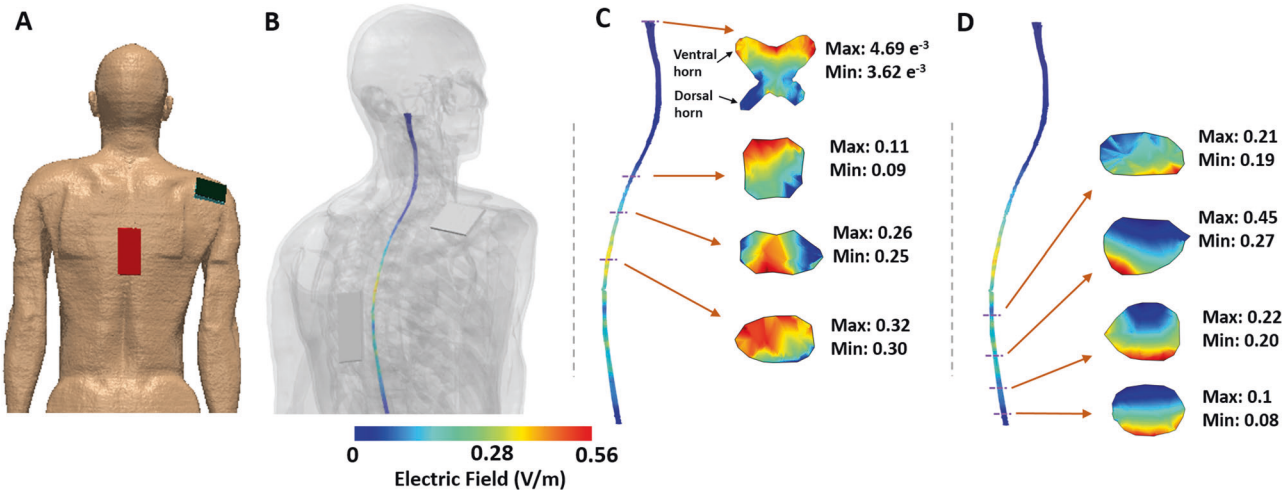

Fig. 3 E-field simulation. Anodal tsDCS at 2.5 mA E-field simulation with thoracic (T10; anode)/right shoulder (cathode) electrode montage. Finite element model geometry is shown in (**A**). Induced E-field strengths (V/m) on spinal gray matter with tissues made semi-transparent (**B**). Selected spinal gray matter 2D slices showing E-field strength (individual segment Min/Max values) above the center of the anode electrode (**C**) and below the anode electrode (**D**). Images (**A**) and (**B**) are shown at different scales.

DATA AVAILABILITY

All study-related data are available upon reasonable request.

REFERENCES

1. Craig AD. How do you feel-now? The anterior insula and human awareness. Nat Rev Neurosci. 2009;10:59–70.
2. Craig AD. Significance of the insula for the evolution of human awareness of feelings from the body. Ann N Y Acad Sci. 2011;1225:72–82.
3. Craig AD. Cooling, pain, and other feelings from the body in relation to the autonomic nervous system. Handb Clin Neurol. 2013;117:103–9.
4. Barrett LF, Simmons WK. Interoceptive predictions in the brain. Nat Rev Neurosci. 2015;16:419–29.
5. Damasio AR. The somatic marker hypothesis and the possible functions of the prefrontal cortex. Philos Trans R Soc Lond B Biol Sci. 1996;351:1413–20.
6. Seth AK, Friston KJ. Active interoceptive inference and the emotional brain. Philos Trans R Soc Lond B Biol Sci. 2016;371:20160007.
7. Kleckner IR, Zhang J, Touroutoglou A, Chanes L, Xia C, Simmons WK, et al. Evidence for a large-scale brain system supporting allostasis and interoception in humans. Nat Hum Behav. 2017;1:0069.
8. Thayer JF, Lane RD. A model of neurovisceral integration in emotion regulation and dysregulation. J Affect Disord. 2000;61:201–16.
9. Craig AD. How do you feel? Interoception: the sense of the physiological condition of the body. Nat Rev Neurosci. 2002;3:655–66.
10. Craig AD. Forebrain emotional asymmetry: a neuroanatomical basis? Trends Cogn Sci. 2005;9:566–71.
11. Strigo IA, Craig AD. Interoception, homeostatic emotions and sympathovagal balance. Philos Trans R Soc Lond B Biol Sci. 2016;371:20160010.
12. Smith R, Kuplicki R, Feinstein J, Forthman KL, Stewart JL, Paulus MP, et al. A Bayesian computational model reveals a failure to adapt interoceptive precision estimates across depression, anxiety, eating, and substance use disorders. PLoS Comput Biol. 2020;16:e1008484.
13. Paulus MP, Stein MB. Interoception in anxiety and depression. Brain Struct Funct. 2010;214:451–63.
14. Furman DJ, Waugh CE, Bhattacharjee K, Thompson RJ, Gotlib IH. Interoceptive awareness, positive affect, and decision making in major depressive disorder. J Affect Disord. 2013;151:780–5.
15. Wiebking C, Bauer A, de Greck M, Duncan NW, Tempelmann C, Northoff G. Abnormal body perception and neural activity in the insula in depression: an fMRI study of the depressed "material me. World J Biol Psychiatry. 2010;11:538–49.
16. Liu CH, Ma X, Song LP, Fan J, Wang WD, Lv XY, et al. Abnormal spontaneous neural activity in the anterior insular and anterior cingulate cortices in anxious depression. Behav Brain Res. 2015;281:339–47.
17. Henje Blom E, Connolly CG, Ho TC, LeWinn KZ, Mobayed N, Han L, et al. Altered insular activation and increased insular functional connectivity during sad and happy face processing in adolescent major depressive disorder. J Affect Disord. 2015;178:215–23.
18. Wiebking C, de Greck M, Duncan NW, Tempelmann C, Bajbouj M, Northoff G. Interoception in insula subregions as a possible state marker for depression—an exploratory fMRI study investigating healthy, depressed and remitted participants. Front Behav Neurosci. 2015;9:82.
19. DeVille DC, Kerr KL, Avery JA, Burrows K, Bodurka J, Feinstein JS, et al. The neural bases of interoceptive encoding and recall in healthy adults and adults with depression. Biol Psychiatry Cogn Neurosci Neuroimaging. 2018;3:546–54.
20. Craig AD. Distribution of trigeminothalamic and spinothalamic lamina I terminations in the macaque monkey. J Comp Neurol. 2004;477:119–48.
21. Polgar E, Wright LL, Todd AJ. A quantitative study of brainstem projections from lamina I neurons in the cervical and lumbar enlargement of the rat. Brain Res. 2010;1308:58–67.
22. Critchley HD, Garfinkel SN. Interoception and emotion. Curr Opin Psychol. 2017;17:7–14.
23. Uddin LQ, Nomi JS, Hebert-Seropian B, Ghaziri J, Boucher O. Structure and function of the human insula. J Clin Neurophysiol. 2017;34:300–6.
24. Engelmann JB, Berns GS, Dunlop BW. Hyper-responsivity to losses in the anterior insula during economic choice scales with depression severity. Psychol Med. 2017;47:2879–91.
25. Wilson RP, Colizzi M, Bossong MG, Allen P, Kempton M, Bhattacharyya S. The neural substrate of reward anticipation in health: a meta-analysis of fMRI findings in the monetary incentive delay task. Neuropsychol Rev. 2018;28:496–506.
26. Pessoa L. Emergent processes in cognitive-emotional interactions. Dialogues Clin Neurosci. 2010;12:433–48.
27. Reisert M, Weiller C, Hosp JA. Displaying the autonomic processing network in humans—a global tractography approach. Neuroimage. 2021;231:117852.
28. Seth AK, Tsakiris M. Being a beast machine: the somatic basis of selfhood. Trends Cogn Sci. 2018;22:969–81.
29. Buijs FN, Leon-Mercado L, Guzman-Ruiz M, Guerrero-Vargas NN, Romo-Nava F, Buijs RM. The circadian system: a regulatory feedback network of periphery and brain. Physiology. 2016;31:170–81.
30. Rodriguez-Cortes B, Hurtado-Alvarado G, Martinez-Gomez R, Leon-Mercado LA, Prager-Khoutorsky M, Buijs RM. Suprachiasmatic nucleus-mediated glucose entry into the arcuate nucleus determines the daily rhythm in blood glycemia. Curr Biol. 2022;32:796–805.e4.
31. Kreier F, Swaab DF. History of hypothalamic research: "the spring of primitive existence". Handb Clin Neurol. 2021;179:7–43.
32. Katsurada K, Kario K. Neural afferents as potential targets to ameliorate FGF21-mediated sympathoexcitation. Hypertens Res. 2022;45:372–5.
33. American Psychiatric Association. Diagnostic and statistical manual of mental disorders. 5th ed. Washington, DC: American Psychiatric Association; 2013.
34. Kennis M, Gerritsen L, van Dalen M, Williams A, Cuijpers P, Bockting C. Prospective biomarkers of major depressive disorder: a systematic review and meta-analysis. Mol Psychiatry. 2020;25:321–38.
35. Stanghellini G, Ballerini M, Fernandez AV, Cutting J, Mancini M. Abnormal body phenomena in persons with major depressive disorder. Psychopathology. 2021;54:203–13.

36. Wiebking C, Northoff G. Neural activity during interoceptive awareness and its associations with alexithymia—an fMRI study in major depressive disorder and non-psychiatric controls. Front Psychol. 2015;6:589.
37. Lenoir C, Jankovski A, Mouraux A. Anodal transcutaneous spinal direct current stimulation (tsDCS) selectively inhibits the synaptic efficacy of nociceptive transmission at spinal cord level. Neuroscience. 2018;393:150–63.
38. Truini A, Vergari M, Biasiotta A, La Cesa S, Gabriele M, Di Stefano G, et al. Transcutaneous spinal direct current stimulation inhibits nociceptive spinal pathway conduction and increases pain tolerance in humans. Eur J Pain. 2011;15:1023–7.
39. Thordstein M, Svantesson M, Rahin H. Effect of transspinal direct current stimulation on afferent pain signalling in humans. J Clin Neurosci. 2020;77:163–7.
40. Parazzini M, Fiocchi S, Liorni I, Rossi E, Cogiamanian F, Vergari M, et al. Modeling the current density generated by transcutaneous spinal direct current stimulation (tsDCS). Clin Neurophysiol. 2014;125:2260–70.
41. Kuck A, Stegeman DF, van Asseldonk EHF. Modeling trans-spinal direct current stimulation for the modulation of the lumbar spinal motor pathways. J Neural Eng. 2017;14:056014.
42. Fritsch B, Reis J, Martinowich K, Schambra HM, Ji Y, Cohen LG, et al. Direct current stimulation promotes BDNF-dependent synaptic plasticity: potential implications for motor learning. Neuron. 2010;66:198–204.
43. Miranda PC, Mekonnen A, Salvador R, Ruffini G. The electric field in the cortex during transcranial current stimulation. Neuroimage. 2013;70:48–58.
44. Nitsche MA, Paulus W. Excitability changes induced in the human motor cortex by weak transcranial direct current stimulation. J Physiol. 2000;527:633–9.
45. Marangolo P, Fiori V, Shofany J, Gili T, Caltagirone C, Cucuzza G, et al. Moving beyond the brain: transcutaneous spinal direct current stimulation in post-stroke aphasia. Front Neurol. 2017;8:400.
46. Bocci T, Caleo M, Vannini B, Vergari M, Cogiamanian F, Rossi S, et al. An unexpected target of spinal direct current stimulation: interhemispheric connectivity in humans. J Neurosci Methods. 2015;254:18–26.
47. Bocci T, Barloscio D, Vergari M, Di Rollo A, Rossi S, Priori A, et al. Spinal direct current stimulation modulates short intracortical inhibition. Neuromodulation. 2015;18:686–93.
48. Tozzi L, Doolin K, Farrel C, Joseph S, O'Keane V, Frodl T. Functional magnetic resonance imaging correlates of emotion recognition and voluntary attentional regulation in depression: a generalized psycho-physiological interaction study. J Affect Disord. 2017;208:535–44.
49. McCreery DB, Agnew WF, Yuen TG, Bullara L. Charge density and charge per phase as cofactors in neural injury induced by electrical stimulation. IEEE Trans Biomed Eng. 1990;37:996–1001.
50. Eldridge SM, Chan CL, Campbell MJ, Bond CM, Hopewell S, Thabane L, et al. CONSORT 2010 statement: extension to randomised pilot and feasibility trials. Pilot Feasibility Stud. 2016;2:64.
51. Sheehan DV, Lecrubier Y, Sheehan KH, Amorim P, Janavs J, Weiller E, et al. The Mini-International Neuropsychiatric Interview (M.I.N.I.): the development and validation of a structured diagnostic psychiatric interview for DSM-IV and ICD-10. J Clin Psychiatry. 1998;59:22–33.
52. Montgomery SA, Asberg M. A new depression scale designed to be sensitive to change. Br J Psychiatry. 1979;134:382–9.
53. Williams JB, Kobak KA. Development and reliability of a structured interview guide for the Montgomery Asberg Depression Rating Scale (SIGMA). Br J Psychiatry. 2008;192:52–8.
54. Trivedi MH, Corey-Lisle PK, Guo Z, Lennox RD, Pikalov A, Kim E. Remission, response without remission, and nonresponse in major depressive disorder: impact on functioning. Int Clin Psychopharmacol. 2009;24:133–8.
55. Posner K, Brown GK, Stanley B, Brent DA, Yershova KV, Oquendo MA, et al. The Columbia-Suicide Severity Rating Scale: initial validity and internal consistency findings from three multisite studies with adolescents and adults. Am J Psychiatry. 2011;168:1266–77.
56. Busner J, Targum SD. The clinical global impressions scale: applying a research tool in clinical practice. Psychiatry. 2007;4:28–37.
57. Kroenke K, Spitzer RL, Williams JB. The PHQ-9: validity of a brief depression severity measure. J Gen Intern Med. 2001;16:606–13.
58. Terluin B, van Marwijk HW, Ader HJ, de Vet HC, Penninx BW, Hermens ML, et al. The Four-Dimensional Symptom Questionnaire (4DSQ): a validation study of a multidimensional self-report questionnaire to assess distress, depression, anxiety and somatization. BMC Psychiatry. 2006;6:34.
59. Gormally J, Black S, Daston S, Rardin D. The assessment of binge eating severity among obese persons. Addict Behav. 1982;7:47–55.
60. Mehling WE, Price C, Daubenmier JJ, Acree M, Bartmess E, Stewart A. The Multidimensional Assessment of Interoceptive Awareness (MAIA). PLoS ONE. 2012;7:e48230.
61. Milaneschi Y, Lamers F, Bot M, Drent ML, Penninx BW. Leptin dysregulation is specifically associated with major depression with atypical features: evidence for a mechanism connecting obesity and depression. Biol Psychiatry. 2017;81:807–14.
62. Li L, Shelton RC, Chassan RA, Hammond JC, Gower BA, Garvey TW. Impact of major depressive disorder on prediabetes by impairing insulin sensitivity. J Diabetes Metab. 2016;7:664.
63. Bookout AL, de Groot MH, Owen BM, Lee S, Gautron L, Lawrence HL, et al. FGF21 regulates metabolism and circadian behavior by acting on the nervous system. Nat Med. 2013;19:1147–52.
64. McNamara RK, Jandacek R, Tso P, Blom TJ, Welge JA, Strawn JR, et al. Adolescents with or at ultra-high risk for bipolar disorder exhibit erythrocyte docosahexaenoic acid and eicosapentaenoic acid deficits: a candidate prodromal risk biomarker. Early Inter Psychiatry. 2016;10:203–11.
65. Datta A, Bansal V, Diaz J, Patel J, Reato D, Bikson M. Gyri-precise head model of transcranial direct current stimulation: improved spatial focality using a ring electrode versus conventional rectangular pad. Brain Stimul. 2009;2:201–7.
66. Bikson M, Datta A. Guidelines for precise and accurate computational models of tDCS. Brain Stimul. 2012;5:430–1.
67. Datta A, Truong D, Minhas P, Parra LC, Bikson M. Inter-individual variation during transcranial direct current stimulation and normalization of dose using MRI-derived computational models. Front Psychiatry. 2012;3:91.
68. Rampersad SM, Janssen AM, Lucka F, Aydin U, Lanfer B, Lew S, et al. Simulating transcranial direct current stimulation with a detailed anisotropic human head model. IEEE Trans Neural Syst Rehabil Eng. 2014;22:441–52.
69. Christ A, Kainz W, Hahn EG, Honegger K, Zefferer M, Neufeld E, et al. The virtual family-development of surface-based anatomical models of two adults and two children for dosimetric simulations. Phys Med Biol. 2010;55:N23–38.
70. Twisk JW, Rijnhart JJ, Hoekstra T, Schuster NA, Ter Wee MM, Heymans MW. Intention-to-treat analysis when only a baseline value is available. Contemp Clin Trials Commun. 2020;20:100684.
71. Woods AJ, Antal A, Bikson M, Boggio PS, Brunoni AR, Celnik P, et al. A technical guide to tDCS, and related non-invasive brain stimulation tools. Clin Neurophysiol. 2016;127:1031–48.
72. Modolo J, Denoyer Y, Wendling F, Benquet P. Physiological effects of low-magnitude electric fields on brain activity: advances from in vitro, in vivo and in silico models. Curr Opin Biomed Eng. 2018;8:38–44.
73. Guidetti M, Giannoni-Luza S, Bocci T, Pacheco-Barrios K, Bianchi AM, Parazzini M, et al. Modeling electric fields in transcutaneous spinal direct current stimulation: a clinical perspective. Biomedicines. 2023;11:1283.
74. Ezquerro F, Moffa AH, Bikson M, Khadka N, Aparicio LV, de Sampaio-Junior B, et al. The influence of skin redness on blinding in transcranial direct current stimulation studies: a crossover trial. Neuromodulation. 2017;20:248–55.
75. Webster RK, Bishop F, Collins GS, Evers AWM, Hoffmann T, Knottnerus JA, et al. Measuring the success of blinding in placebo-controlled trials: should we be so quick to dismiss it? J Clin Epidemiol. 2021;135:176–81.

ACKNOWLEDGEMENTS

This study was funded by the Brain and Behavior Research Foundation NARSAD Young Investigator Award (#26649) issued to FRN. FRN was also partially funded by a National Institute of Mental Health K23 Award (K23MH120503). REDCap at the University of Cincinnati is funded by the National Institutes of Health (NIH) Clinical and Translational Science Award (CTSA) program, grant UL1TR001425. We would like to thank all participants. The authors also acknowledge Brian Martens for his contributions during the study. Results included in this manuscript were presented in part as an oral presentation at the Society of Biological Psychiatry annual meeting 2023 held in San Diego, CA. A poster related to this work was presented at the 2023 National Network of Depression Centers (NNDC) annual conference in Houston. A preprint is posted on MedRxiv https://doi.org/10.1101/2023.05.20.23290247.

AUTHOR CONTRIBUTIONS

FRN, OOA, SLM, RMB, RKM, MPD, LRP, and JW contributed to conceptualization and methodology. FRN, OOA, AIG, GG, NM, RKM, and SLM contributed to investigation. FRN, TJB, and JW contributed to formal analysis and visualization of clinical trial data. FRN, AD, and AG conceptualized or generated the analysis and visualization of the E-field model. FRN, OOA, IB, TJB, JW, DEF, MPD, RKM, RMB, MAF, and SLM contributed to writing the original draft. All authors contributed to review and editing of the final manuscript.

COMPETING INTERESTS

FRN receives grant support from the National Institute of Mental Health K23 Award (K23MH120503) and from a 2017 NARSAD Young Investigator Award from the Brain and Behavior Research Foundation; is the inventor of U.S. Patent and Trademark Office patent # 10,857,356, transcutaneous spinal cord stimulation for treatment of psychiatric disorders; with the University of Cincinnati as assignee. The potential for a conflict of interest during the study was disclosed and addressed by UC's IRB. FRN has also received

consultant fees from Otsuka Pharmaceutical and non-financial research support from Soterix Medical. Soterix Medical provided non-financial research support consisting in a secondary transcutaneous spinal direct current stimulator device in loan during the study. Soterix Medical did not participate in the planning, design, conduction, analysis, or interpretation of the clinical trial data. AD and AG work in Research and Development at Soterix Medical and contributed to generate the E-field simulation presented in this manuscript. OOA reports grant support from the American Academy of Neurology Institute and has no potential conflict of interest with this study. IB, TJB and JW report no conflict of interest. AD is supported by grants from the National Institute of Health (NIH): 75N95020C00024 and 1R44MH126833-01A1, Department of Defense (DOD): W912CG21C0014, and National Aeronautics and Space Administration (NASA): 80NSSC22CA071. AD and AG are employees of Soterix Medical, Inc. AIG is a consultant for SignantHealth. DEF, GG, NM and LRP report no conflict of interest. MPD has received research support from the National Institute of Health, the Patient-Centered Outcomes Research Institute (PCORI), AbbVie, Alkermes, Eli Lilly, Janssen, Johnson and Johnson, Lundbeck, Myriad, Novartis, Otsuka, Pfizer, Sage, Shire, Sunovion, Supernus, and Vanda and has provided consultation or advisory board services for Alkermes, Allergan, Assurex, CMEology, Janssen, Johnson and Johnson, Lundbeck, Myriad, Neuronetics, Otsuka, Pfizer, and Sage. RKM and RMB report no conflict of interest. MAF has received grant support from Assurex Health and Mayo Foundation, has received CME travel support and honoraria from Carnot Laboratories and American Physician Institute, and has financial interest/stockownership/royalties with Chymia LLC. SLM is or has been a consultant to or member of the scientific advisory boards of F. Hoffmann-La Roche Ltd. Idorsia, Myriad, Novo Nordisk, Otsuka, Sipnose, Sunovion and Takeda. She is or has been a principal or co-investigator on studies sponsored by Brainsway, Idorsia, Janssen, Marriott Foundation, Myriad, National Institute of Mental Health, Novo Nordisk, Otsuka, and Sunovion. She is also an inventor on United States Patent No. 6,323,236 B2, Use of Sulfamate Derivatives for Treating Impulse Control Disorders, and along with the patent's assignee, University of Cincinnati, Cincinnati, Ohio, has received payments from Johnson & Johnson, which has exclusive rights under the patent.

ADDITIONAL INFORMATION

Supplementary information The online version contains supplementary material available at https://doi.org/10.1038/s41380-023-02349-9.

Correspondence and requests for materials should be addressed to Francisco Romo-Nava.

Reprints and permission information is available at http://www.nature.com/reprints

Publisher's note Springer Nature remains neutral with regard to jurisdictional claims in published maps and institutional affiliations.